Hindawi
International Journal of Analytical Chemistry
Volume 2019, Article ID 5970754, 10 pages
https://doi.org/10.1155/2019/5970754

Research Article

Preparation of Monodisperse Enrofloxacin Molecularly Imprinted Polymer Microspheres and Their Recognition Characteristics

Xiaoxiao Wang,[1] Yanqiang Zhou,[1] Yuling Niu,[2] Shanwen Zhao,[1] and Bolin Gong[1]

[1]*College of Chemistry and Chemical Engineering, North Minzu University, Yinchuan 750021, China*
[2]*Ningxia Entry-Exit Inspection and Quarantine Bureau Comprehensive Technology Center, Yinchuan, Ningxia, China*

Correspondence should be addressed to Bolin Gong; gongbolin@163.com

Received 27 December 2018; Revised 2 February 2019; Accepted 5 March 2019; Published 1 April 2019

Academic Editor: Bogusław Buszewski

This study presents a new strategy for the detection of enrofloxacin (ENR) in food samples by the use of monodisperse ENR molecularly imprinted polymers (MIPs). Using enrofloxacin as template molecule, methacrylic acid as functional monomer, and ethylene diglycidyl ether as cross-linker, surface molecularly imprinted polymers (MIPs) were prepared on the surface of polymeric glycidyl methacrylate-ethylene glycol dimethacrylate ($P_{GMA\text{-}EDMA}$) microspheres. The surface morphology and imprinting behavior of $P_{GMA\text{-}EDMA}$@MIPs were investigated and optimized. Synthesized $P_{GMA\text{-}EDMA}$@MIPs showed good physical and chemical stability and specific recognition toward fluoroquinolones. The introduction of $P_{GMA\text{-}EDMA}$ microspheres greatly increased the adsorption area of $P_{GMA\text{-}EDMA}$@MIPs and increased the adsorption capacity of target molecules. The core shell structure increased the adsorption rate, and adsorption equilibrium was achieved within 6 min, much higher than that of MIPs synthesized by traditional methods. Enrofloxacin in milk samples was detected by molecular imprinting solid phase extraction (MISPE) combined with high performance liquid chromatography (HPLC). Implementing this method resulted in a recovery rate of 94.6~109.6% with a relative standard deviation (RSD) of less than 3.2%. The limit of detection (LOD) of this method was identified as three times the signal-to-noise ratio (10 μg/L). In summary, this work proposed a sensitive, rapid, and convenient method for the determination of trace ENR in food samples.

1. Introduction

Enrofloxacin (ENR) is an antibiotic belonging to the fluoroquinolone class (FQs) of synthetic antibiotics. The physicochemical properties and broad spectrum of activity of FQs antibiotics against most bacteria have led to their widespread use in human medicine, as well as the prevention and treatment of animal diseases in livestock [1–3]. However, trace amounts of these drugs can be detected in food products taken from animals treated with FQs antibiotics, posing a threat to human health (such as toxicity, drug resistance, and anaphylaxis) [4]. In fact, many countries have established a maximum limit of FQs residues in food. Additionally, the environmental impact of FQs residues has recently attracted worldwide attention. Therefore, sensitive and selective method for the detection and quantification of FQs is an important area of research. The currently available methods for the detection of FQs in different environments consist of high performance liquid chromatography [5] coupled to mass spectrometry [6, 7], ultraviolet (UV) [8], and fluorescence detection[9, 10]. However, the complex matrices of biological samples present challenges for the selective quantification of trace amounts of FQs in food products.

Molecularly imprinted technology (MIT) [11–13] is a method that can be used to develop polymers for the selective identification of a particular molecular target or a class of molecules [14]. To prepare the polymer, a functional monomer is constructed with binding sites matching the shape, size, and functional groups of a template molecule. The functional monomers are then copolymerized and cross-linked in the presence of the template molecule to create a polymer network capable of molecular recognition. Subsequent removal of the template molecules from the polymer network facilitates the selective binding and recognition of

the template molecule or structural analogs in a sample mixture [15]. MIPs are attractive materials for molecular recognition due to their low cost, simple preparation, high stability, and good reproducibility under harsh chemical and physical conditions. Consequently, MIT has been widely used in extraction separation [16, 17], chemical sensing [18], catalysis [19], and chiral separations [20–22]. Surface molecular imprinting distributes almost all binding sites on a surface with good accessibility by taking some measures, which facilitates the removal and recombination of template molecules. This method is therefore particularly suitable for the preparation of imprinted polymers of biomacromolecules. The distribution of binding sites across the polymer surface shortens the adsorption equilibrium time by overcoming the traditional embedding phenomenon [23, 24].

The preparation of MIPs using ENR as a template molecule has been recently explored in the literature; the resulting MIPs would have important implications for the selective detection of ENR in complex matrices. Xiao *et al.* [25] prepared FQs imprinted polymers on the surface of magnetic carbon nanotubes and simultaneously used a pseudo template to achieve fluoroquinolone extraction. Additionally, work by He *et al.* [26] firstly attempted to prepare an ENR imprinted material using the magnetic polyhedral oligomeric semi-siloxane composite as a matrix. In a similar vein, Yan *et al.* [27] thermally initiated polymerization of the monolithic column and use norfloxacin as a pseudo template for ENR; the resulting material demonstrated a high affinity for ENR and norfloxacin in water and successfully afforded the extraction of ENR and norfloxacin from blood samples. Despite these great advancements in the development of MIPs, the preparation of monodisperse ENR imprinted polymers by surface grafting and the application of the resultant polymers to a real sample analysis have yet to be reported.

In this work, self-made monodisperse macroporous cross-linked polymeric glycidyl methacrylate-ethylene glycol dimethacrylate ($P_{GMA\text{-}EDMA}$) microspheres are used as the matrix. Compared with silica gel and other carriers, it is more resistant to acid and alkaliand has a large number of active groups on the surface. It is an ideal molecularly imprinted carrier. A surface grafting technique was used to prepare enrofloxacin molecular imprinted polymers attached to the surface of $P_{GMA\text{-}EDMA}$ microspheres via MPS modified sites. The surface structure and the physicochemical properties of the polymers were analyzed and used for the detection of four FQs in milk samples.

2. Materials and Method

2.1. Reagent and Instrument. Enrofloxacin (ENR), tetracycline (TC), ofloxacin (OFL), chloramphenicol (CAP), glycidyl methacrylate (GMA), ethylene glycol dimethacrylate (EDMA), ethylene glycol diglycidyl ether (EGDE), methacrylic acid (MAA), ammonium persulfate [$(NH_4)_2S_2O_8$], 3-methacryloylpropyl trimethoxysilane (MPS), styrene (St), azobisisobutyronitrile (AIBN), polyvinylpyrrolidone (PVP), cyclohexanol, poly(vinyl alcohol) (PVA), dibutyl phthalate (DBP), ethyl alcohol, pyridine, methanol, acetone, acetic acid, sodium dodecyl sulfate(SDS),and tetrahydrofuran (THF) were purchased from Aladdin Reagent (Shanghai, China). HPLC grade methanol and acetonitrile were obtained from Sigma (St. Louis, MO, USA). Milk samples were purchased from a local supermarket. The polymerization inhibitor was removed from the MAA by using a vacuum distillation unit. Water was twice distilled prior to use. All other reagents were of analytical grade and used without further purification unless otherwise specified. All solutions prepared for HPLC were filtered through a 0.45μm nylon filter before use.

Chromatography was performed using an LC-20AT chromatographic system (Shimadzu, Japan) equipped with two LC-20AT pumps and a SPD-20A UV–VIS detector. Samples were injected through a Rheodyne 7725 valve. Polymers morphology was characterized by using a JSM-7500F electron scanning microscope (JEOL Co., Japan). Elemental analysis was performed on a VarioEL III elemental analyzer (Elementar Co., Germany). Infrared spectra were collected by using a Fourier transform infrared spectrometer (Shimadzu, Japan). Absorption spectra were collected by using a TU-1810-type ultraviolet spectrophotometer (Beijing General Instrument Co., Ltd., China). Centrifugation was performed with a TG16-WS high-speed centrifuge (Centrifuge Factory, China).

2.2. Preparation of Monodisperse $P_{GMA\text{-}EDMA}$ Microspheres. Monodisperse polystyrene seeds (PS) were synthesized according to a dispersion polymerization method. The monomer styrene (10 mL), initiator ABIN (0.2 g), stabilizer PVP (2 g), and anhydrous ethanol (87.8 mL) were combined in a 100 mL single-necked flask and sonicated until all of the styrene, ABIN, and PVP were dissolved. The flask was then attached to a rotary device equipped with a heating apparatus. Polymerization was carried out at 70°C over the course of 24 h. Upon completion of the reaction, the solvent was removed by centrifugation and the remaining solids were washed with copious amounts of ethanol to obtain the desired PS.

In a 150 mL single-necked flask, GMA (6 mL), ABIN (0.36 g), EDMA (6 mL), DBP (6 mL), and cyclohexanol (6 mL) were combined and sonicated to dissolve completely; then 45 mL distilled water, 75 mL 0.2% SDS solution, and 35 mL 5% PVA solution were added to the above mixed solution. The reaction mixture was subjected to ultrasonic emulsification for 30 min until complete emulsification of the organic phase was achieved. The resultant emulsion was slowly added to a solution of the prepared monodisperse PS while the temperature was maintained at 30°C. The reaction mixtures were stirred for 24 h, then degassed under a nitrogen atmosphere for 20 min, and still stirred at 70°C for additional 24 h. The solids obtained were washed with water, methanol, and acetone and then dried in vacuo to yield the product. The porogens were removed by extraction with tetrahydrofuran for 48 h in a Soxhlet apparatus for products. The products were washed with methanol again and dried in vacuo to yield the $P_{GMA\text{-}EDMA}$ microspheres.

$P_{GMA\text{-}EDM}$ (2.0 g) were suspended in 100 mL of 0.1 mol/L sulfuric acid, stirred, and kept at 60°C for 12 h. Then the products were filtered and washed with water until neutral and then dried under vacuum to afford the hydrolyzed $P_{GMA\text{-}EDMA}$ microspheres.

2.3. Preparation of $P_{GMA\text{-}EDMA}$@MIPs

2.3.1. Bonding of MPS on the Surface of $P_{GMA\text{-}EDMA}$. The hydrolyzed microspheres $P_{GMA\text{-}EDMA}$ (2.0 g) were ultrasonically dispersed in 100 mL of 50% (V/V) ethanol. MPS (2.5 mL) and pyridine (3 drops) were added to the dispersion and the mixtures were heated to 50°C for 24 h. Unreacted silylation reagent was removed from the mixture by vacuum filtration using absolute ethanol. The products were concentrated in vacuo to obtain the modified microspheres $P_{GMA\text{-}EDMA}$@MPS.

2.3.2. Grafting MAA on $P_{GMA\text{-}EDMA}$@MPS. The $P_{GMA\text{-}EDMA}$@MPS (2.0 g) microspheres and MAA (7 mL) were combined in 150 mL of water and $(NH4)_2S_2O_8$ (0.042 g) were added as an initiator for the graft polymerization reaction. The reactant mixtures were heated to 70°C for 24 h, while constantly stirring under an atmosphere of nitrogen. The resultant microspheres were purified by Soxhlet extraction in ethanol to remove unreacted MAA physically attached to the microspheres. The solution was dried in vacuo to yield the grafted $P_{GMA\text{-}EDMA}$@MPS@MAA microspheres.

2.3.3. Preparation of MIPs. The $P_{GMA\text{-}EDMA}$@MPS@MAA (2.0 g) microspheres were dissolved in 50mL 10 mmol/L ENR methanol solution. The mixtures were shaken at 25°C for 6 h until the adsorption of ENR by $P_{GMA\text{-}EDMA}$@MPS@MAA reached equilibrium. The reactant mixtures were then filtered and the ENR-adsorbed microspheres $P_{GMA\text{-}EDMA}$@MPS@MAA were dried under vacuum. The ENR-adsorbed $P_{GMA\text{-}EDMA}$@MPS@MAA microspheres (2.0 g) were added to 50mL 4 mmol/L ENR 50 % aqueous methanol solution. The pH of the solution was adjusted to 8.0 using NaOH solution and then EGDE (2.5 mL) was added as a cross-linker. The reactant mixture was stirred at 50°C for 8 h to complete polymerization. After the reaction finished, the product was washed with methanol and dried at 60°C. The MIP material was extracted with Soxhlet using methanol/acetic acid (9/1, v/v) mixture to remove the unreacted cross-linker EGDE and residual template. The non-imprinted polymers ($P_{GMA\text{-}EDMA}$@NIPs) were synthesized according to the same procedures described above except in the absence of a template molecule.

2.4. Adsorption Experiments. To measure the adsorption capacity of the polymers, the $P_{GMA\text{-}EDMA}$@MIPs (20 mg) was mixed with a series of methanol solutions of ENR at various concentrations. Each reactant mixture was shaken for 12 h and then subjected to centrifugation. Supernatant was quantified by UV spectrometry at 280 nm and then the adsorption amount was calculated according to

$$Q = \frac{(C_0 - C_e)\,V}{m} \tag{1}$$

where Q (mg/g) represents the mass of ENR adsorbed per gram of polymer, C_o (mg/L) and C_e (mg/L) are the initial and final concentrations of ENR in solution, respectively, V (L) is the total volume of the solution, and m (g) is the mass of polymer.

For the kinetic experiments, the $P_{GMA\text{-}EDMA}$@MIPs (20 mg) was added to a methanol solution of ENR (10 mL, 2 mM). The series of prepared reaction mixtures were mechanically shaken for different lengths of adsorption time at room temperature, after which each of the mixtures was subjected to centrifugation to afford separation. Supernatant was quantified by UV spectrometry at 280 nm and then the adsorption amount was calculated according to (1).

The operation procedures of $P_{GMA\text{-}EDMA}$@NIPs were the same as those of $P_{GMA\text{-}EDMA}$@MIPs.

2.5. Selective Adsorption Experiments. To investigate the selectivity of the prepared $P_{GMA\text{-}EDMA}$@MIPs towards ENR, the binding of ENR was tested in comparison to three structural analogs: ofloxacin (OFL), tetracycline (TC), and chloramphenicol (CAP) (Figure 1). The $P_{GMA\text{-}EDMA}$@MIPs (20 mg) was added to flasks containing methanol solutions (10 mL, 2 mM) of ENR. The shaking adsorption process was carried out for 12 h at 25°C. The adsorption capacity of $P_{GMA\text{-}EDMA}$@MIPs to OFL, TC, and CAP was determined in the same way. The operation procedures of $P_{GMA\text{-}EDMA}$@NIPs were the same as those of $P_{GMA\text{-}EDMA}$@MIPs.

The distribution coefficients (K_D), selectivity coefficients (k), relative selectivity coefficients (k'), and imprinting factor (α) of OTC and CTC with respect to TC can be obtained according to the following equations:

$$K_D = \frac{Q_e}{C_e} \tag{2}$$

$$k = \frac{K_{D(FQs)}}{K_{D(TC)}} \tag{3}$$

$$k' = \frac{K_{MIPs}}{K_{NIPs}} \tag{4}$$

$$\alpha = \frac{Q_{MIPs}}{Q_{NIPs}} \tag{5}$$

where Q_e (mg/g) and C_e (mg/L) represent the amount of binding and concentration of substrate at equilibrium, respectively. $K_{D(FQS)}$ represents the distribution coefficients of the fluoroquinolones, $K_{D(TC)}$ represents the distribution coefficients of the tetracyclines, and K_{MIPs} and K_{NIPs} are the selectivity coefficients of the $P_{GMA\text{-}EDMA}$@MIPs and $P_{GMA\text{-}EDMA}$@NIPs, respectively. Q_{MIPs} and Q_{NIPs} represent the adsorption capacity of the $P_{GMA\text{-}EDMA}$@MIPs and $P_{GMA\text{-}EDMA}$@NIPs for ENR, respectively.

2.6. Spiked Recovery Experiments and Analysis of Actual Samples. A sample of milk (0.5 mL) solution was combined with acetonitrile (0.5 mL) solution homogenized. This mixture solution contained ENR and its concentration was 0.025 mmol/L. The samples were centrifuged for 5 min at a speed of 10000 rpm. The supernatant was collected and diluted with phosphate buffer solution (PBS, PH 6, 0.25 mM) to 10 mL.

A SPE column filled with $P_{GMA\text{-}EDMA}$@MIPs or $P_{GMA\text{-}EDMA}$@NIPs was activated with methanol (2 mL) and pure water (2 mL), successively. The spiked milk sample (3 mL) was flowed through the column, and then

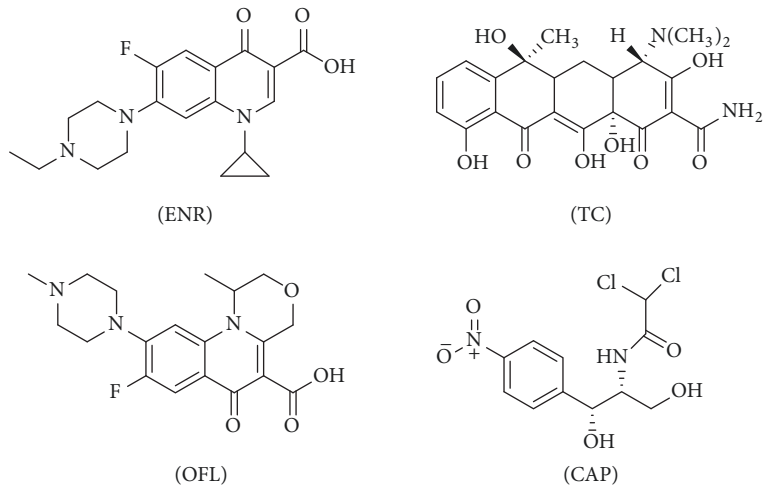

Figure 1: The structures of ENR, TC, OFL, and CAP.

a methanol/acetic acid (9/1, v/v) solution (3 mL) was used to elute the extracted analytes. The collected eluate was concentrated by N_2 stream and then dissolved again with 1 mL mobile phase. Finally, 20 μL samples were detected by HPLC (LC-20AT, Shimadzu corporation). Chromatographic conditions: stationary phase: C_{18} reversed phase chromatographic column (150 mm×4.6 mm, Agilent Corporation, USA); Mobile phase: 0.025mol/L phosphoric acid solution (adjust PH to 3.0 with triethylamine.) (A)~acetonitrile (B). Flow rate: 0.8 mL/min; The detection wavelength is 278 nm by UV detector.

3. Results and Discussion

3.1. Preparation of Enrofloxacin-Imprinted $P_{GMA\text{-}EDMA}$@MIPs. To introduce polymerizable double bonds to the surface of the $P_{GMA\text{-}EDMA}$ microspheres for facile preparation of the $P_{GMA\text{-}EDMA}$@MIPs, the microsphere surface was modified with coupling agent MPS. Polymerization was initiated to graft the functional monomer MAA to the surface of microspheres, and the resultant $P_{GMA\text{-}EDMA}$@MPS@MAA microspheres were saturated to adsorb ENR. By adding the cross-linker EGDE, to the microspheres under alkaline conditions, a ring-opening reaction between the epoxy group on the cross-linking agent and the carboxyl group on the $P_{GMA\text{-}EDMA}$@MPS@MAA macromolecule forms a network, which encapsulated the ENR molecule, and thereby gained ENR molecularly imprinted polymer. The ENR was then extracted from the $P_{GMA\text{-}EDMA}$@MIPs using a methanol/acetic acid (9/1, v/v) mixture, creating holes in the thin layer of the polymer well matched for the size and intermolecular interactions required for ENR binding. The preparation of the $P_{GMA\text{-}EDMA}$@MIPs is summarized in Figure 2.

3.2. Characterization of Enrofloxacin-Imprinted $P_{GMA\text{-}EDMA}$@MIPs. FT-IR analysis of $P_{GMA\text{-}EDMA}$@MIPs and the precursor materials is shown in Figure 3. The hydrolyzed $P_{GMA\text{-}EDMA}$ microspheres exhibit a strong absorption peak at 1727 cm^{-1} corresponding to the stretching vibration of carbonyl grafted to the microsphere, characteristic -CH stretching vibrations are noted at 2955 cm^{-1}, and an -OH stretching vibration is noted at 2955 cm^{-1} as a broad absorption peak. The preparation of $P_{GMA\text{-}EDMA}$@MPS depends on the reaction of the silanylated reagent, MPS with hydroxyl groups of the microsphere surface; the observed decrease in the intensity of the characteristic -OH peak at 3525 cm^{-1} in $P_{GMA\text{-}EDMA}$@MPS relative to the precursor microspheres is attributed to the partial consumption of the surface -OH functional groups. The spectra of the $P_{GMA\text{-}EDMA}$@MIPs show an increase in intensity of a peak around 1093 cm^{-1}, corresponding to -C-O-C stretching vibrations in the EGDE cross-linker. Moreover, the absorption peak at 3525 cm^{-1} is enhanced due to the reaction of the carboxyl groups of $P_{GMA\text{-}EDMA}$@MIPs with the epoxy groups on the cross-linker molecules, which generates additional free hydroxyl groups.

The SEM analysis of the $P_{GMA\text{-}EDMA}$@MIPs and precursor $P_{GMA\text{-}EDMA}$ microspheres are depicted in Figure 4. The left image in Figure 4 is an SEM image of the $P_{GMA\text{-}EDMA}$ microspheres; the surface of $P_{GMA\text{-}EDMA}$ microsphere is divided into uniform pores, formed during the one-step seed swelling and polymerization process used for microsphere preparation. A comparison of the SEM image of the $P_{GMA\text{-}EDMA}$ microspheres with that of the $P_{GMA\text{-}EDMA}$@MIPs prepared by surface modification (Figure 4, right) reveals the presence of regular gaps in the surface of the $P_{GMA\text{-}EDMA}$@MIPs, created upon removal of the template molecule. The particle size of $P_{GMA\text{-}EDMA}$@MIPs is about 5 μm and its surface is porous.

The $P_{GMA\text{-}EDMA}$ microspheres and $P_{GMA\text{-}EDMA}$@MPS and $P_{GMA\text{-}EDMA}$@MIPs microspheres were characterized by elemental analysis. The results of these measurements are listed in Table 1. The elemental analysis reveals an increase in carbon content of $P_{GMA\text{-}EDMA}$@MPS to the starting material $P_{GMA\text{-}EDMA}$, indicating a successful grafting of MPS to the surface of the microspheres. The data for the $P_{GMA\text{-}EDMA}$@MIPs indicates an increase in both nitrogen and carbon composition. This increase in N/C content is consistent with the successful grafting of the cross-linking agent EGDE to the surface of the microspheres.

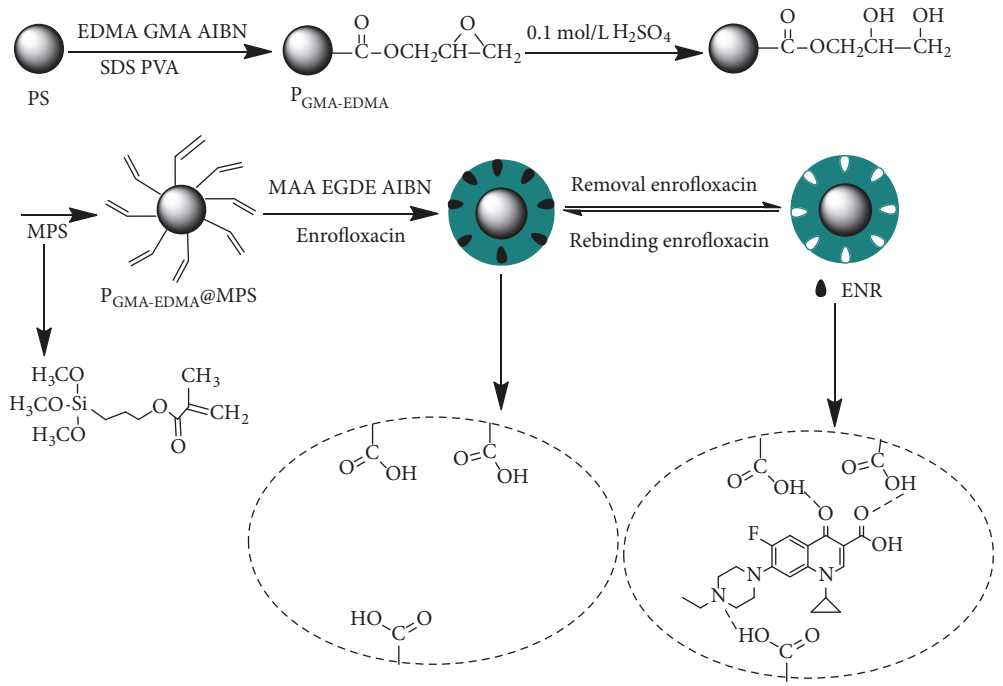

Figure 2: Schematic expression of the reaction process used to prepare $P_{GMA-EDMA}$@MIPs.

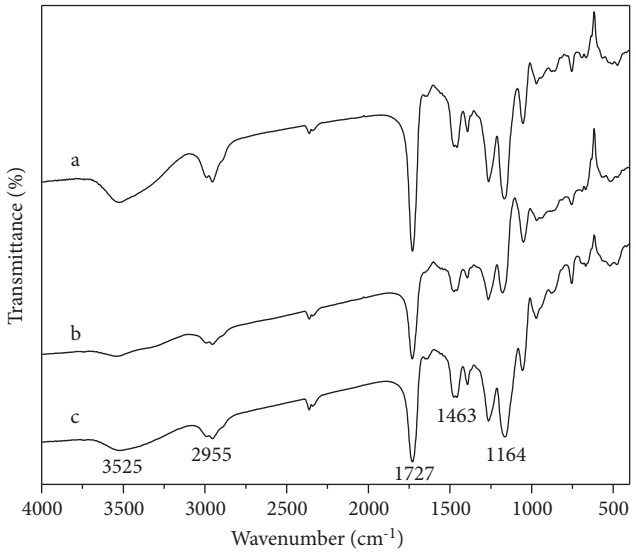

Figure 3: FT-IR spectra of $P_{GMA/EDMA}$ (a), $P_{GMA/EDMA}$@MPS (b), and $P_{GMA-EDMA}$@MIPs (c).

Table 2 shows the specific surface area, pore volume, and average pore size of $P_{GMA-EDMA}$, $P_{GMA-EDMA}$@MIPs, and $P_{GMA-EDMA}$@NIPs from nitrogen adsorption-desorption analysis. As can be seen from (Table 2), the specific surface area of $P_{GMA-EDMA}$@MIPs decreases markedly with respect to $P_{GMA-EDMA}$, which is due to the fact that $P_{GMA-EDMA}$@MIPs is based on $P_{GMA-EDMA}$ to prepare imprinted polymer. $P_{GMA-EDMA}$@MIPs have larger specific surface area, pore volume, and average pore size than $P_{GMA-EDMA}$@NIPs. The results showed that the different adsorption properties of $P_{GMA-EDMA}$@MIPs and $P_{GMA-EDMA}$@NIPs could not only be completely attributed to the difference in morphology but also be related to the imprinting process that produced specific recognition sites. Larger pore volume and average pore size provide complementary spatial structures for selective recognition of template molecules and competitors with $P_{GMA-EDMA}$@MIPs.

3.3. Absorption Performance

3.3.1. Absorption Capacity and Kinetics. The adsorption isotherm data of the $P_{GMA-EDMA}$@MIPs were analyzed using Scatchard [28] model and processed according to the following equation:

$$\frac{Q}{C_e} = -\frac{Q}{K_d} + \frac{Q_{max}}{K_d} \quad (6)$$

where Q and Q_{max} are the experimental adsorption capacity to the template ENR(mg/g) and the theoretical maximum adsorption capacity of the polymer (mg/g), respectively; C_e is the concentration of ENR in equilibrium in solution (mg/L) after adsorption and K_d is the dissociation constant (mg/L).

The Scatchard model was implemented on the adsorption isotherm data of the $P_{GMA-EDMA}$@MIPs and $P_{GMA-EDMA}$@NIPs and the Scatchard figure created by plotting Q against Q/Ce (Figure 5). The Scatchard analysis curve of the $P_{GMA-EDMA}$@MIPs consists of two lines with different slopes, while the Scatchard analysis curve of the $P_{GMA-EDMA}$@NIPs is in a straight line, suggesting the fact that while the $P_{GMA-EDMA}$@NIPs only has a single binding site for ENR, $P_{GMA-EDMA}$@MIPs exhibits two distinct binding sites. One of the binding sites of the $P_{GMA-EDMA}$@MIPs is a nonspecific

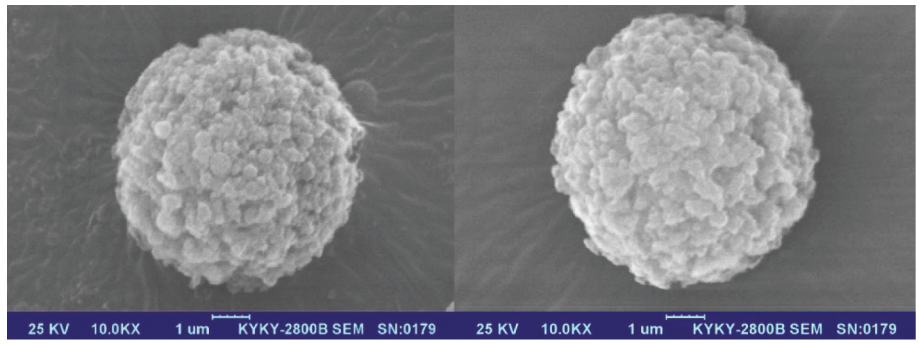

Figure 4: Scanning electron micrographs of $P_{GMA\text{-}EDMA}$ microspheres and $P_{GMA\text{-}EDMA}$@MIPs.

Table 1: Elemental analysis results of $P_{GMA\text{-}EDMA}$@MIPs.

Samples	Elemental composition (%)		
	C	N	H
$P_{GMA\text{-}EDMA}$	54.95	0.329	6.599
$P_{GMA\text{-}EDMA}$@MPS	55.48	0.233	6.442
$P_{GMA\text{-}EDMA}$@MIPs	55.87	0.506	5.599

Table 2: Comparison of $P_{GMA\text{-}EDMA}$ and $P_{GMA\text{-}EDMA}$@MIPs from nitrogen adsorption-desorption analysis.

Sample	Surface area /($m^2 \bullet g^{-1}$)	Pore Volume /($cm^3 \bullet g^{-1}$)	Average Pore Size /(nm)
$P_{GMA\text{-}EDMA}$	150.58	0.930	11.92
$P_{GMA\text{-}EDMA}$@MIPs	103.43	0.72	24.92
$P_{GMA\text{-}EDMA}$@NIPs	85.02	0.56	8.60

Table 3: The results of the Scatchard analysis of $P_{GMA\text{-}EDMA}$@MIPs.

Binding site	Linear equation	K_d (mg/L)	Q_{max} (mg/g)
Low affinity	Q/C_e =-0.0009511Q+0.0825(R=0.9842)	1051.43	86.74
High affinity	Q/C_e=-0.00429Q+0.1203 (R=0.9183)	233.10	28.05

adsorption site similar to that in $P_{GMA\text{-}EDMA}$@NIPs formed by hydrophobic, hydrogen bonds and physical adsorption, while the other is the high affinity specific recognition site created by the imprinted hole. The additional binding site of the $P_{GMA\text{-}EDMA}$@MIPs is responsible for the higher adsorption capacity and better selectivity of this system relative to the $P_{GMA\text{-}EDMA}$@NIPs.

The values of K_d and Q_{max} are calculated from the slope and intercept of the linear segments in the Scatchard plots, respectively. The parameters defining $P_{GMA\text{-}EDMA}$@MIPs were obtained from the slope and intercept of Scatchard curve, and the results are shown in (Table 3). The K_d and Q_{max} values were similarly calculated for the $P_{GMA\text{-}EDMA}$@NIPs to be 2261.60 mg/L and 55.00 mg/g, respectively.

Plots of the adsorption kinetics of the $P_{GMA\text{-}EDMA}$@MIPs in 2 mM solution of ENR are shown in Figure 6. A rapid adsorption of ENR by the $P_{GMA\text{-}EDMA}$@MIPs up to 90.5% of the adsorption equilibrium is noted within the first 5 min, after which a significant decrease in the adsorption rate occurs. The adsorption equilibrium reached at 6 min. Conversely, adsorption by the $P_{GMA\text{-}EDMA}$@NIPs was slow within the first 3 min, where the driving force of adsorption has non-covalent interactions between ENR and $P_{GMA\text{-}EDMA}$@NIPs. The enhanced binding of ENR by $P_{GMA\text{-}EDMA}$@MIPs is dependent on the interaction between ENR and the imprinted holes of the $P_{GMA\text{-}EDMA}$@MIPs generated on the surface of microspheres during preparation. From the kinetic data, it is noted that the specific adsorption by $P_{GMA\text{-}EDMA}$@MIPs occurs largely in the initial stage of adsorption.

The adsorption isotherm of ENR in the range of 0.125-2.25 mM was obtained by static equilibrium adsorption. The absorption curves showed in Figure 7 show that the adsorption of $P_{GMA\text{-}EDMA}$@MIPs gradually increased with increases in ENR concentration, while rapid saturation was observed in the adsorption by $P_{GMA\text{-}EDMA}$@NIPs. Adsorption by the $P_{GMA\text{-}EDMA}$@MIPs was significantly greater than that of $P_{GMA\text{-}EDMA}$@NIPs at a given concentration. The low adsorption capacity of the $P_{GMA\text{-}EDMA}$@NIPs was attributed to the weak interactions that form between the $P_{GMA\text{-}EDMA}$@NIPs and substrate; substrate binding interactions were derived from the nonspecific adsorption of the polar groups on the $P_{GMA\text{-}EDMA}$@NIPs surface to ENR. In addition to nonspecific adsorption interactions, $P_{GMA\text{-}EDMA}$@MIPs also contained holes matching the spatial structure and complementing the functional groups of ENR. The holes in the

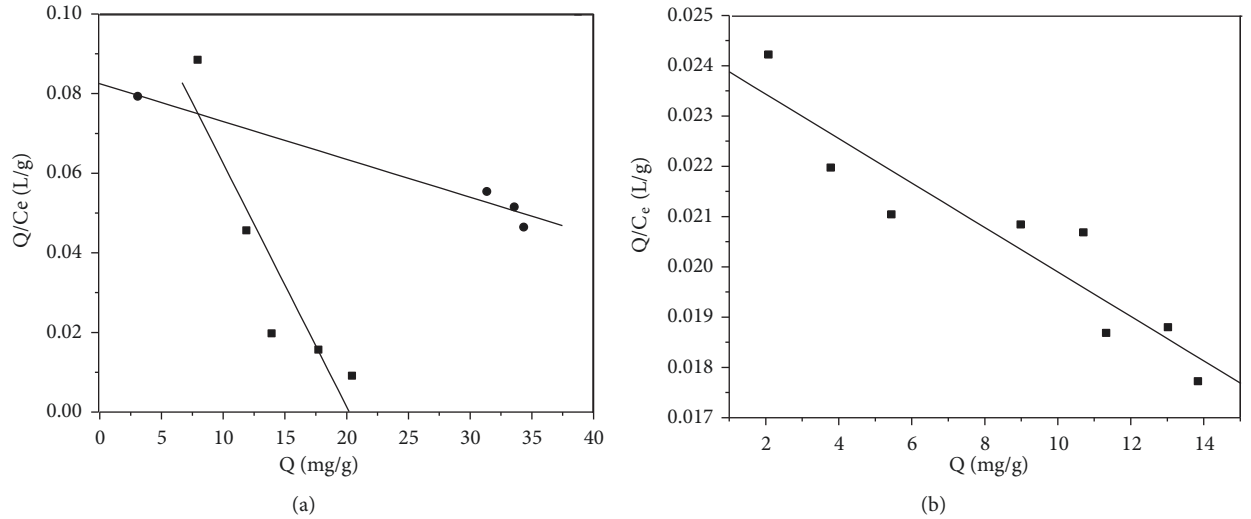

Figure 5: Scatchard analysis plot of the binding of ENR to the $P_{GMA\text{-}EDMA}$@MIPs (a) and $P_{GMA\text{-}EDMA}$@NIPs (b).

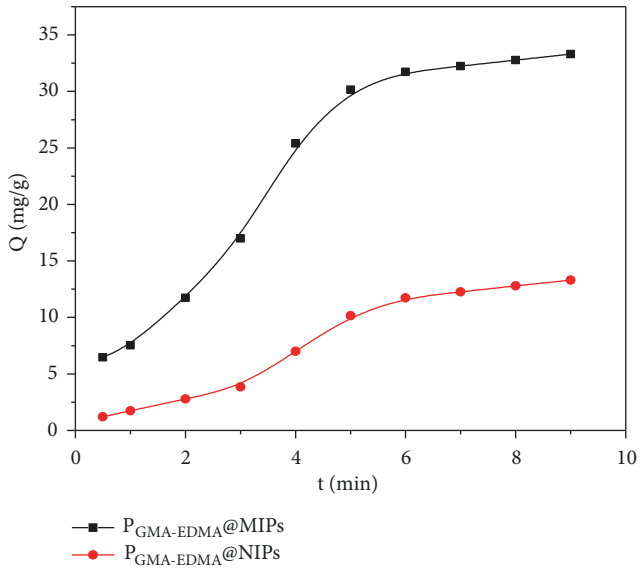

Figure 6: Dynamic adsorption curves of $P_{GMA\text{-}EDMA}$@MIPs and $P_{GMA\text{-}EDMA}$@NIPs.

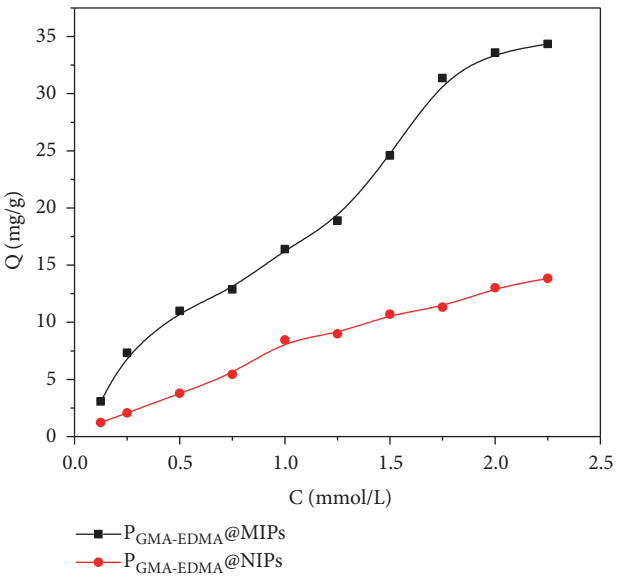

Figure 7: Adsorption isotherm of $P_{GMA\text{-}EDMA}$@MIPs and $P_{GMA\text{-}EDMA}$@NIPs.

$P_{GMA\text{-}EDMA}$@MIPs surface had a memory function for the ENR molecule, and the difference in the adsorption amount of the $P_{GMA\text{-}EDMA}$@MIPs and $P_{GMA\text{-}EDMA}$@NIPs polymers was largely attributed to the specific adsorption of these holes.

3.3.2. Absorption Selectivity. As it can be seen from the data presented in Table 4 and Figure 8, the distribution coefficient K_d, selectivity coefficient k, imprinting factor α, and relative selectivity coefficient k' of adsorbent can be determined via competitive binding experiments. As predicted, the adsorption of ENR and its structural analogues by the $P_{GMA\text{-}EDMA}$@MIPs was greater than that by the $P_{GMA\text{-}EDMA}$@NIPs. The selectivity coefficient (k) defines the selectivity of an absorber over the template molecule. The k values of the $P_{GMA\text{-}EDMA}$@MIPs were all greater than the corresponding values for the $P_{GMA\text{-}EDMA}$@NIPs, suggesting a higher affinity of the $P_{GMA\text{-}EDMA}$@MIPs for the template's structural analogues than for other types of antibiotic [29]. Moreover, the relative selectivity coefficient k' values were all greater than 1, indicating that after removal of the template molecule, holes and special imprinting sites were formed on the polymer surface complementing the shape and functional groups of the template molecule. Among ENR and its structural analogues, $P_{GMA\text{-}EDMA}$@MIPs has the largest imprinting factor α value for ENR, which indicates that $P_{GMA\text{-}EDMA}$@MIPs has stronger affinity and excellent selectivity for ENR.

3.4. Analysis of Real Samples. Solid phase extraction is afforded via a four-step process: activation, loading, leaching,

Table 4: The selective coefficient of the $P_{GMA\text{-}EDMA}$@MIPs and $P_{GMA\text{-}EDMA}$@NIPs.

Analyte	Q (mg/g)		K_d (mL/g)		k		α	k'
	MIPs	NIPs	MIPs	NIPs	MIPs	NIPs		
ENR	33.58	6.02	46.72	18.12	3.56	3.50	5.58	1.02
OFL	23.70	5.56	32.79	7.69	2. 50	1.49	4.26	1.67
TC	11.67	4.60	13.13	5.17	—	—	2.53	—
CAP	4.97	1.77	7.69	2. 74	—	—	2.80	—

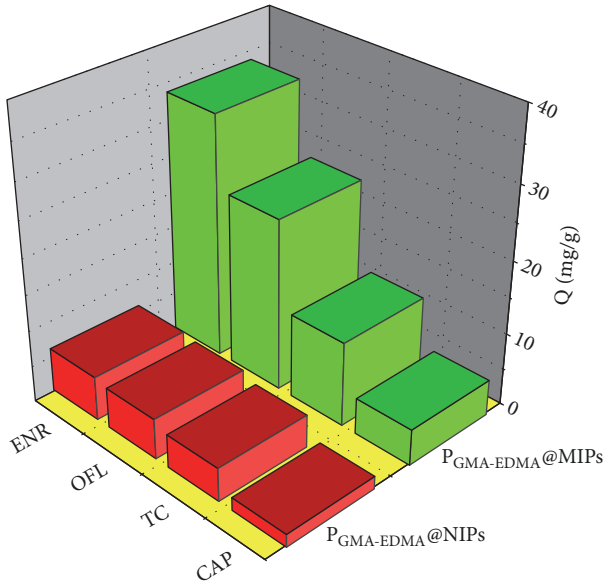

Figure 8: Binding isotherms of ENR, OFL, TC, and CAP on the $P_{GMA\text{-}EDMA}$@MIPs and $P_{GMA\text{-}EDMA}$@NIPs.

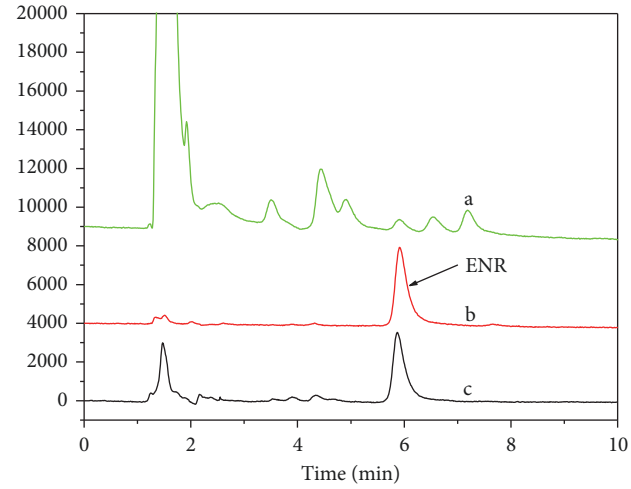

Figure 9: The chromatogram of milk samples: (a) initial milk sample, (b) sample after $P_{GMA\text{-}EDMA}$@MIPs treatment, and (c) sample after C_{18}-SPE treatment.

and eluting. Using water (3 mL) as leachate effectively removes the endogenous components of biological samples, as demonstrated in Figure 9. Following C_{18} extraction, the variance in the recovery of interfering substances was attributed to the type of nonspecific interaction between the different components in the sample matrix and the C_{18} adsorbent, such as the difference between hydrophobic versus hydrophilic interactions. In molecularly imprinted polymer solid-phase extraction (MISPE), the $P_{GMA\text{-}EDMA}$@MIPs has better selectivity for the target substrate, resulting in high recovery and a purer extraction.

A standard curve for ENR detection was established over the concentration range 100.0~900.0 μg/L to yield an expression of y=132741x+740.35 and a correlation coefficient of R=0.9986. Milk samples were spiked with ENR standard solutions with concentrations of 100 μg/L, 200 μg/L, and 500 μg/L. As demonstrated in Table 5, the rate of recovery of the ENR from these samples measured between 94.6 and 109.6% upon extraction with the $P_{GMA\text{-}EDMA}$@MIPs, with a relative standard deviation (RSD) between 1.1 and 3.2%. The minimum limit of detection (LOD) was determined to be 10 μg/L by tripling the signal-to-noise ratio. (Table 6) summarizes the results of the existing reports on the detection of ENR in the milk samples by different types of ENR imprinted materials. These results demonstrate a high recovery rate for methodology of this study.

4. Conclusions

A novel core-shell $P_{GMA\text{-}EDMA}$@MIPs was prepared for simultaneous separation and enrichment of four FQs in milk samples. As $P_{GMA\text{-}EDMA}$ is easy to modify, stable physicochemical and thermal stability, easily controllable synthesis conditions, low cost, small nonspecific adsorption, and so on, the prepared $P_{GMA\text{-}EDMA}$@MIPs had the advantages of stable properties, high selectivity, and recovery rate. $P_{GMA\text{-}EDMA}$@MIPs have been successfully applied to the enrichment and separation of FQs in milk samples. This work provides a versatile approach for fabricating well-constructed core-shell $P_{GMA\text{-}EDMA}$@MIPs particles for rapid enrichment and highly selective separation of target molecules in real samples.

Data Availability

The data used to support the findings of this study are included within the paper.

Ethical Approval

This paper does not contain any studies with human participants or animals performed by any of the authors.

Table 5: Recoveries and RSDs of SPE-HPLC method for the spiked milk samples.

	Added concentration/μg L^{-1}	Recoveries (%)	RSD (%)
MIP	100	94.6	2.9
	200	95.6	3.2
	500	109.6	1.1
C_{18}	100	72.6	4.0
	200	75.6	3.2
	500	78.3	4.4

Table 6: Comparison of the ENR-MIPs applied for milk samples' TCs detection with existing reports.

Preparing methods	Test method	Analyte	Linearity range/μg·L^{-1}	Limit of detection/μg·L^{-1}	Recoveries/%	References
Surface imprinting	HPLC-UV	ENR, PEF	2.5–500	0.7	92.04-98.31	[29]
Surface imprinting	HPLC-UV	ENR, OFL, DAN	50–1000	1.76-12.42	75.6–108.9	[28]
Bulk polymerization	HPLC-UV	ENR, CIP	—	6 5	82.6–93.5	[30]
Sacrificial surface imprinting	HPLC-UV	OFL, ENR, NOR	30–250	—	90.9-102.1	[31]

Conflicts of Interest

We declare that we have no financial and personal relationships with other people or organizations that can inappropriately influence our work. The authors have declared no conflicts of interest.

Authors' Contributions

Xiaoxiao Wang and Yanqiang Zhou contributed equally to this work.

Acknowledgments

This work was financially supported by the National Natural Science Foundation of China (no. 21565001 and no. 31271868), Key Project of North Minzu University (2015KJ30).

References

[1] M. Pan, Y. Gu, M. Zhang, J. Wang, Y. Yun, and S. Wang, "Reproducible molecularly imprinted QCM sensor for accurate, stable, and sensitive detection of enrofloxacin residue in animal-derived foods," *Food Analytical Methods*, vol. 11, no. 2, pp. 495–503, 2017.

[2] W. P. da Silva, L. H. de Oliveira, A. L. D. Santos, V. S. Ferreira, and M. A. G. Trindade, "Sample preparation combined with electroanalysis to improve simultaneous determination of antibiotics in animal derived food samples," *Food Chemistry*, vol. 250, pp. 7–13, 2018.

[3] Y. Tang, M. Li, X. Gao et al., "Preconcentration of the antibiotic enrofloxacin using a hollow molecularly imprinted polymer, and its quantitation by HPLC," *Microchimica Acta*, vol. 183, no. 2, pp. 589–596, 2016.

[4] Y. Tang, M. Li, X. Gao et al., "A NIR-responsive up-conversion nanoparticle probe of the $NaYF_4$:Er,Yb type and coated with a molecularly imprinted polymer for fluorometric determination of enrofloxacin," *Microchimica Acta*, vol. 184, no. 9, pp. 3469–3475, 2017.

[5] M. J. Schneider, A. M. Darwish, and D. W. Freeman, "Simultaneous multiresidue determination of tetracyclines and fluoroquinolones in catfish muscle using high performance liquid chromatography with fluorescence detection," *Analytica Chimica Acta*, vol. 586, no. 1-2, pp. 269–274, 2007.

[6] F. Yu, S. Yu, L. Yu et al., "Determination of residual enrofloxacin in food samples by a sensitive method of chemiluminescence enzyme immunoassay," *Food Chemistry*, vol. 149, pp. 71–75, 2014.

[7] Y. Xiao, H. Chang, A. Jia, and J. Hu, "Trace analysis of quinolone and fluoroquinolone antibiotics from wastewaters by liquid chromatography–electrospray tandem mass spectrometry," *Journal of Chromatography A*, vol. 1214, no. 1-2, pp. 100–108, 2008.

[8] M. Lillenberg, S. Yurchenko, K. Kipper et al., "Simultaneous determination of fluoroquinolones, sulfonamides and tetracyclines in sewage sludge by pressurized liquid extraction and liquid chromatography electrospray ionization-mass spectrometry," *Journal of Chromatography A*, vol. 1216, no. 32, pp. 5949–5954, 2009.

[9] A. Poliwoda, M. Krzyzak, and P. P. Wieczorek, "Supported liquid membrane extraction with single hollow fiber for the analysis of fluoroquinolones from environmental surface water samples," *Journal of Chromatography A*, vol. 1217, no. 22, pp. 3590–3597, 2010.

[10] Y.-B. Luo, Q. Ma, and Y.-Q. Feng, "Stir rod sorptive extraction with monolithic polymer as coating and its application to the analysis of fluoroquinolones in honey sample," *Journal of Chromatography A*, vol. 1217, no. 22, pp. 3583–3589, 2010.

[11] B. Sellergren, "Imprinted polymers with memory for small molecules, proteins, or crystals," *Angewandte Chemie International Edition*, vol. 39, no. 6, pp. 1031–1037, 2000.

[12] B. Gao, J. Wang, F. An, and Q. Liu, "Molecular imprinted material prepared by novel surface imprinting technique for selective adsorption of pirimicarb," *Polymer Journal*, vol. 49, no. 5, pp. 1230–1238, 2008.

[13] Y. R. Gong, Y. Wang, J. B. Dong et al., "Preparation of isoprocarb surface molecular-imprinted materials and its recognition character," *Chinese Journal of Analytical Chemistry*, vol. 42, no. 1, pp. 28–35, 2014.

[14] H. Yan, F. Qiao, and H. R. Kyung, "Molecularly imprinted-matrix solid-phase dispersion for selective extraction of five fluoroquinolones in eggs and tissue," *Analytical Chemistry*, vol. 79, no. 21, pp. 8242–8248, 2007.

[15] Y. Niu, C. Liu, J. Yang et al., "Preparation of tetracycline surface molecularly imprinted material for the selective recognition of tetracycline in milk," *Food Analytical Methods*, vol. 9, no. 8, pp. 2342–2351, 2016.

[16] Y. Hu, J. Pan, K. Zhang, H. Lian, and G. Li, "Novel applications of molecularly-imprinted polymers in sample preparation," *TrAC - Trends in Analytical Chemistry*, vol. 43, pp. 37–52, 2013.

[17] A. Martín-Esteban, "Molecularly-imprinted polymers as a versatile, highly selective tool in sample preparation," *TrAC - Trends in Analytical Chemistry*, vol. 45, pp. 169-170, 2013.

[18] M. Trojanowicz, "Enantioselective electrochemical sensors and biosensors: A mini-review," *Electrochemistry Communications*, vol. 38, pp. 47–52, 2014.

[19] J. Zhang, M. Zhang, K. Tang, F. Verpoort, and T. Sun, "Polymer-based stimuli-responsive recyclable catalytic systems for organic synthesis," *Small*, vol. 10, no. 1, pp. 32–46, 2014.

[20] F. Rong, X. Feng, C. Yuan, D. Fu, and P. Li, "Chiral separation of mandelic acid and its derivatives by thin-layer chromatography using molecularly imprinted stationary phases," *Journal of Liquid Chromatography & Related Technologies*, vol. 29, no. 17, pp. 2593–2602, 2006.

[21] J. Yin, G. Yang, and Y. Chen, "Rapid and efficient chiral separation of nateglinide and its l-enantiomer on monolithic molecularly imprinted polymers," *Journal of Chromatography A*, vol. 1090, no. 1-2, pp. 68–75, 2005.

[22] R. J. Ansell, "Molecularly imprinted polymers for the enantioseparation of chiral drugs," *Advanced Drug Delivery Reviews*, vol. 57, no. 12, pp. 1809–1835, 2005.

[23] Y. Li, X. Li, C. Dong, J. Qi, and X. Han, "A graphene oxide-based molecularly imprinted polymer platform for detecting endocrine disrupting chemicals," *Carbon*, vol. 48, no. 12, pp. 3427–3433, 2010.

[24] Y. Li, X. Li, C. Dong, Y. Li, P. Jin, and J. Qi, "Selective recognition and removal of chlorophenols from aqueous solution using molecularly imprinted polymer prepared by reversible addition-fragmentation chain transfer polymerization," *Biosensors and Bioelectronics*, vol. 25, no. 2, pp. 306–312, 2009.

[25] D. Xiao, P. Dramou, N. Xiong et al., "Preparation of molecularly imprinted polymers on the surface of magnetic carbon nanotubes with a pseudo template for rapid simultaneous extraction of four fluoroquinolones in egg samples," *Analyst*, vol. 138, no. 11, pp. 3287–3296, 2013.

[26] H.-B. He, C. Dong, B. Li et al., "Fabrication of enrofloxacin imprinted organic-inorganic hybrid mesoporous sorbent from nanomagnetic polyhedral oligomeric silsesquioxanes for the selective extraction of fluoroquinolones in milk samples," *Journal of Chromatography A*, vol. 1361, pp. 23–33, 2014.

[27] H. Yan, F. Qiao, and K. H. Row, "Molecularly imprinted monolithic column for selective on-line extraction of enrofloxacin and ciprofloxacin from urine," *Chromatographia*, vol. 70, no. 7-8, pp. 1087–1093, 2009.

[28] Y. Hiratsuka, N. Funaya, H. Matsunaga, and J. Haginaka, "Preparation of magnetic molecularly imprinted polymers for bisphenol A and its analogues and their application to the assay of bisphenol A in river water," *Journal of Pharmaceutical and Biomedical Analysis*, vol. 75, pp. 180–185, 2013.

[29] X. Sun, X. Tian, Y. Zhang, and Y. Tang, "Molecularly imprinted layer-coated silica gel particles for selective solid-phase extraction of pefloxacin and enrofloxacin from milk samples," *Food Analytical Methods*, vol. 6, no. 5, pp. 1361–1369, 2013.

[30] H. Yan, M. Tian, and K. H. Row, "Determination of enrofloxacin and ciprofloxacin in milk using molecularly imprinted solid-phase extraction," *Journal of Separation Science*, vol. 31, no. 16-17, pp. 3015–3020, 2008.

[31] W. J. Tang, T. Zhao, C. H. Zhou, X. J. Guan, and H. X. Zhang, "Preparation of hollow molecular imprinting polymer for determination of ofloxacin in milk," *Analytical Methods*, vol. 6, no. 10, pp. 3309–3315, 2014.